*Supported by National Science Foundation.

†Based on a thesis submitted by E. S. Chang to the faculty of the University of California, Riverside, in partial fulfillment of the requirements of the Ph.D. degree (1967). Portions of this work were reported briefly at the New York meeting of the American Physical Society; Bull. Am. Phys. Soc. 12, 68 (1967).

‡Present address: Laboratory for Theoretical Studies, Goddard Space Flight Center, NASA, Greenbelt, Maryland.

[1]D. A. Goodings, Phys. Rev. 123, 1706 (1961).

[2]R. E. Watson and A. J. Freeman, Phys. Rev. 123, 2027 (1961); N. Bessis, H. Lefebvre-Brion, C. M. Moser, A. J. Freeman, R. K. Nesbet, and R. E. Watson, Phys. Rev. 135, A588 (1964).

[3]V. Heine, Czech. J. Phys. B13, 619 (1963).

[4]C. M. Sachs, Phys. Rev. 117, 1504 (1960).

[5]W. Marshall, Proc. Phys. Soc. (London) A78, 113 (1961); J. Phys. Soc. Japan 17, Suppl. B-I, 20 (1962).

[6]E. A. Hylleraas, Z. Physik 54, 347 (1929).

[7]H. M. James and A. S. Coolidge, Phys. Rev. 49, 688 (1936); 55, 873 (1939).

[8]A. W. Weiss, Phys. Rev. 122, 1826 (1961).

[9]H. P. Kelly, Phys. Rev. 131, 684 (1963); 136, B896 (1964); 144, 39 (1966).

[10]R. T. Pu and E. S. Chang, Phys. Rev. 151, 31 (1966).

[11]M. H. Cohen, D. A. Goodings, and V. Heine, Proc. Phys. Soc. (London) 73, 811 (1959).

[12]G. D. Gaspari, W. M. Shyu, and T. P. Das, Phys. Rev. 134, A852 (1964).

[13]K. F. Berggren and R. F. Wood, Phys. Rev. 130, 198 (1963).

[14]J. Goldstone, Proc. Roy. Soc. (London) A239, 267 (1957).

[15]C. C. J. Roothaan, L. M. Sachs, and A. W. Weiss, Rev. Mod. Phys. 32, 186 (1960); E. Clementi, IBM J. Res. Develop. 9, 2 (1965).

[16]R. Marriott, Proc. Phys. Soc. (London) 72, 121 (1958).

[17]M. G. Salvadori and M. L. Baron, Numerical Methods in Engineering (Prentice-Hall, Inc., Englewood Cliffs, N. J., 1961).

[18]C. W. Cooley, Math. Computations 15, 363 (1961).

[19]E. Fermi, Z. Physik 60, 320 (1930).

[20]N. F. Ramsey, Nuclear Moments (John Wiley & Sons, Inc., New York; Chapman & Hall, Ltd., London, 1953).

[21]R. H. Lambert and F. M. Pipkin, Phys. Rev. 128, 198 (1962).

[22]N. F. Ramsey, Molecular Beams (Oxford University Press, 1956).

[23]R. K. Nesbet, Quantum Theory of Atoms, Molecules, Solid States (Academic Press, Inc., New York, 1966).

[24]C. L. Pekeris, Phys. Rev. 112, 1649 (1958); 115, 1216 (1959).

[25]C. W. Scherr, N. J. Silverman, and F. A. Matsen, Phys. Rev. 127, 830 (1962), see Tables V and VI.

[26]E. A. Burke, Phys. Rev. 135, A621 (1964).

[27]R. K. Nesbet, Phys. Rev. 118, 681 (1960).

[28]R. K. Nesbet, in Proceedings of the International Colloquium No. 164 on the Magnetic Hyperfine Structure of Atoms and Molecules, Paris, 1966 (Centre National de la Recherche Scientifique, 1967), p. 87; for other energy calculations with Bethe-Goldstone method, see R. K. Nesbet, Phys. Rev. 155, 56 (1967).

PHYSICAL REVIEW VOLUME 174, NUMBER 1 5 OCTOBER 1968

Many-Body Calculation of Atomic Polarizability -Relation to Hartree-Fock Theory*

Edward S. Chang,† Robert T. Pu, and T. P. Das
Department of Physics, University of California, Riverside, California
(Received 6 November 1967)

The Brueckner-Goldstone perturbation method has been applied to the calculation of the dipole polarizability (α_d) and antishielding factor (γ_d) for lithium-atom ground state. The complete set of states utilized is the same as those employed in earlier calculations of the hyperfine constant and correlation energy. Our results are $\alpha_d = 24.84$ Å^3 and $\gamma_d = 0.958$, as compared to a recent experimental value for $\alpha_d = 22 \pm 2$ Å^3 and $\gamma_d = 1.000$ from the Hellmann-Feynman theorem. The relationship between the Brueckner-Goldstone and the Hartree-Fock perturbation procedures is discussed with reference to specific physical effects.

I. INTRODUCTION

In an earlier paper,[1] referred to as I, we have applied the Brueckner-Goldstone[2] (BG) formalism to the study of the hyperfine constant and the energy of lithium as a test of the atomic ground-state wave function. In the present work, we shall investigate the atomic dipole polarizability (α_d) and the induced electric field at the nucleus which is characterized by the shielding factor (γ_d), both of which have been studied earlier for beryllium and oxygen atoms by Kelly.[3,4] These properties require the ground-state wave function as well as the perturbed wave function in an external field, and therefore provide additional test of the unperturbed wave function. Our aim in the present work is twofold; first, to utilize the diagrammatic technique to study the relative importance of various physical effects that contribute to the polarizability, similar to our earlier analysis of the hyperfine in-

teraction; and second, to establish the relationship between the BG and the conventional HF perturbation theory in the various approximations. Among the physical factors that contribute to the polarizability are: first, the intrinsic effect connected with the individual perturbation of the orbitals; second, the self-consistency effect; and third, the correlation effect.

The physical implication of self-consistency in the present situation is that the distortion of each electronic orbital is influenced by that of other orbitals through the averaged Coulomb and exchange potentials produced by them. Correlation is interpreted as the dynamic dependence of one electron on another. In the language of many-body theory, the former is represented by single-particle excitations and the latter by two- or more-particle excitations. We will show that Hartree-Fock perturbation theory does include some two-body excitations. Since conventionally the Hartree-Fock theory, however, is defined so as to include only self-consistency effects, we define correlation in the presence of an external perturbation as the two- or more-body excitations neglected by usual Hartree-Fock theory. The conventional Hartree-Fock perturbation procedures as summarized by Langhoff, Karplus, and Hurst[5] (LKH) necessarily neglect correlation effects which present no additional difficulties to the BG method. Thus the calculation of α_d and γ_d by the BG procedure allows one to evaluate the importance of correlation effects in the wave function in the peripheral and the central regions of the atom.

We have chosen the lithium atom as the example with which to study the features of the BG procedure primarily for three reasons. The polarizability of the lithium atom has been measured quite accurately, contrary to the situation in beryllium and oxygen where no experimental values are currently available. Secondly, since the properties of the lithium atom have been extensively studied earlier,[5,6] meaningful comparisons can be carried out between the BG results and previous ones. Furthermore, we have made use of the same complete set of states for both the present calculations and the earlier ones on energy and hfs. The over-all results would thus be expected to shed light on the question of the feasibility of obtaining a variety of properties of an atom using the BG procedure with the same complete set of states.

II. BRUECKNER-GOLDSTONE PERTURBATION METHOD –RELATION TO HARTREE-FOCK THEORY

The perturbation Hamiltonian for an atom in a uniform electric field $\vec{E}$ is given by

$$H'' = \sum_{i=1}^{N} h_i' = -E \sum_{i=1}^{N} r_i P_1(\cos\theta_i) \tag{1}$$

where $\vec{r}_i = (r_i, \theta_i, \varphi_i)$ represents the coordinates of the ith electron with respect to the nucleus, the z axis being taken along the direction of E. The summation runs over the N electrons in the atom. From usual perturbation theory considerations, the polarizability is given by

$$\alpha = -2\langle\Psi_0|H''|\Psi_1\rangle/\langle\Psi_0|\Psi_0\rangle, \tag{2}$$

where Ψ_0 is the exact free-atom wave function and Ψ_1 the first-order perturbation in the wave function due to H''. Similarly the induced electric field at the nucleus due to the perturbed electrons is given by

$$E_{\text{ind}} = E\gamma_d = -2\langle\Psi_0|\gamma_{\text{op}}|\Psi_1\rangle/\langle\Psi_0|\Psi_0\rangle, \tag{3}$$

$$\text{where } \gamma_{\text{op}} = \sum_{i=1}^{N} P_1(\cos\theta_i)/r_i^2. \tag{4}$$

The quantity γ_d has often been referred to as the dipole shielding factor in the literature. By the Hellmann-Feynman theorem,[7] $\gamma_d = 1$ for the neutral lithium atom.

The free-atom Hamiltonian H can be separated into two parts

$$H = H_0 + H' \tag{5}$$

$$\text{with } H_0 = \sum_{i=1}^{N} T_i + \sum_{i=1}^{N} V_i$$

$$H' = \sum_{i<j}^{N} v_{ij} - \sum_{i=1}^{N} V_i, \tag{6}$$

$$\text{where } T_i = -\tfrac{1}{2}\nabla_i^2 - z/r_i \tag{7}$$

$$v_{ij} = 1/|\vec{r}_i - \vec{r}_j|, \tag{8}$$

and V_i is a suitably chosen one-electron potential. The two choices of interest in this work, V^N and V^{N-1}, have been discussed by Kelly[3] and are defined below in terms of their matrix elements:

$$\langle p|V^N|i\rangle = \sum_{n=1}^{N} (\langle pn|v|in\rangle - \langle pn|v|ni\rangle) \tag{9}$$

and

$$\langle p|V^{N-1}|i\rangle = \sum_{n=1}^{N-1} (\langle pn|v|in\rangle - \langle pn|v|ni\rangle). \tag{10}$$

The states N are chosen to be the lowest Hartree-Fock states, whereas the states p and i satisfy Eq. (11) as explained in I.

$$(T+V)\phi_i = \epsilon_i\phi_i \ . \tag{11}$$

There are two important differences between the V^N and V^{N-1} potentials. The V^N potential reproduces all the one-electron Hartree-Fock wave functions for the atom, while the V^{N-1} potential reproduces the Hartree-Fock wave function for only the $i = N$ state omitted in the summation in Eq. (10). The more crucial point of difference between the two potentials is in the nature of the higher states they generate. The V^N potential leads only to continuum higher states while V^{N-1} produces both bound and continuum states. The presence of these bound states in the complete set is desirable since they resemble the actual excitations of the atom more closely.

In the BG method the exact free-atom wave function Ψ_0 is obtained from Φ_0 by the linked-cluster expansion[2] (described in I)

$$\Psi_0 = \sum_{n=0}^{\infty} L\left(\frac{1}{E_0 - H_0} H'\right)^n \Phi_0, \tag{12}$$

where L means that only linked diagrams are to be included. Similarly the function perturbed once by H'' is given by[3]

$$\Psi_1 = \sum_{n=0}^{\infty} \sum_{m=0}^{\infty} L\left(\frac{1}{E_0 - H'_0} H'\right)^n \times \left(\frac{1}{E_0 - H_0} H''\right)\left(\frac{1}{E_0 - H_0} H'\right)^m \Phi_0. \tag{13}$$

That is, the expansion includes all possible linked diagrams with H'' occurring in any relative time order to the H's. The diagrams for Ψ_0 have been given in previous papers. Diagrams for Ψ_1 involving zero and first order in H' are given in Fig. 1, where we have used ---• for H'', and are classified according to their physical meanings. Diagram (a) represents the intrinsic perturbation of the one-electron states by the external field. It is seen that diagrams (b)–(g) and their corresponding exchange diagrams will sum to zero if V in Eq. (7) is chosen as V^N. However, for a different choice of V, some residual diagrams will remain and they will be called HF correction diagrams.[8] Diagrams (h) and (i) are interpreted as representing self-consistency effects among electrons p and q. Finally, diagrams (j) and (k) seem to represent correlation effects, since they involve simultaneous excitation of two electrons. However, the physical significance of these two diagrams will be further discussed later in this section.

For the choice of $V^N - 1$ as applied to Li, diagrams (b)–(g) will not contribute when the unexcited state i is the $2s$ state. On the other hand, when both i and j are $1s$ states, the residual diagrams $k = 2s$ and the corresponding exchange diagrams must be included. These can be summed to all orders by the shifted-energy denominator technique[3,4]

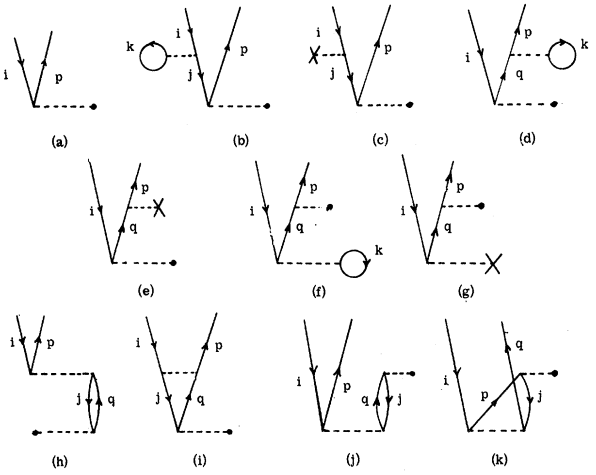

FIG. 1. Diagrams for Ψ_1 involving zero and one order in H'. p and q are unexcited states while i and j denote excited states.

to correct this $1s$ to the HF $1s^0$ state. This HF correction is assumed to be included whenever it applies in future discussions.

In order to justify our interpretation of diagrams, we now discuss the relationship of the perturbation theory to the conventional Hartree-Fock perturbation theory. We recall the fully coupled HF perturbation equations, referred by LKH as Method a.[5] The identical forms, called Eqs. (8a) and (8b) by LKH, are given below:

$$[h^0(1) - \epsilon_i]\phi_i'(1) + [h_i'(1) - \epsilon_i']\phi_i(1) + \sum_{j=1}^{N} [\langle \phi_j' | \frac{1}{r_{12}}(1 - P_{12}) | \phi_j \rangle + \langle \phi_j | \frac{1}{r_{12}}(1 - P_{12}) | \phi_j' \rangle]\phi_i(1) = 0 \tag{14a}$$

$$[h_i^0(1) - \epsilon_i]\phi_i'(1) + [h_i'(1) - \epsilon_i']\phi_i(1) + \sum_{\substack{j=1 \\ j \neq i}}^{N} [\langle \phi_j' | \frac{1}{r_{12}}(1 - P_{12}) | \phi_j \rangle + \langle \phi_j | \frac{1}{r_{12}}(1 - P_{12}) | \phi_j' \rangle]\phi_i(1) = 0, \tag{14b}$$

where $$h^0(1) = T_1 + \sum_{j=1}^{N} \langle \phi_j | \frac{1}{r_{12}}(1 - P_{12}) | \phi_j \rangle \tag{15a}$$

or $$h_i^0(1) = T_1 + \sum_{\substack{j=1 \\ j \neq i}}^{N} \langle \phi_j | \frac{1}{r_{12}}(1 - P_{12}) | \phi_j \rangle \tag{15b}$$

is the one-electron HF Hamiltonian, φ_i the HF orbitals, and φ_i' the perturbed orbitals. P_{12} is a permutation operator introduced to include exchange. Notice that

$$h^0 = T + V^N, \tag{16a}$$

$$h_i^0 = T_i + V_i^{N-1}, \tag{16b}$$

when i is the highest-state N. The uncoupled approximation termed Method b by LKH is obtained by neglecting all terms involving $\varphi j'$ in Eq. (14b) for $\varphi i'$.

$$[h_i^0(1) = -\epsilon_i]\varphi_i'(1) + [h'(1) - \epsilon_i']\varphi_i(1) = 0. \tag{17}$$

Similarly Method c is obtained from Eq. (14a)

$$[h^0(1) - \epsilon_i]\varphi_i'(1) + [h'(1) - \epsilon_i']\varphi_i(1) = 0. \tag{18}$$

Clearly Method c is equivalent to the BG procedure in keeping only the lowest-order diagram, Fig. 1(a), where the states q and j are solutions of Eq. (11) with the choice[4] $V = V^N$. It is easy to see that Method b is equivalent to the same diagram with appropriate corrections but with the

choice[4] $V=V^{N-1}$. In Methods b and c only the intrinsic contributions of the individual electrons contribute to the polarizability, therefore diagram (a) is called intrinsic, and diagrams (b)-(g) HF correction, as discussed previously. LKH observed that Method c includes an extraneous self-potential term which does not arise in Method b. In the BG diagrammatic language, this term can be identified with the self-coupling diagrams (h) and (i) when $i=j$ with $V=V^N$. However, when $V=V^{N-1}$, the diagrams (i) and (h) for $i=j=N$ are cancelled by the residue of diagram (d) and its exchange. When $i\neq j$ in (h) and (i), these diagrams represent the self-consistency terms which appear in Method a but not Methods b and c. (The expansion of the perturbed orbitals in terms of the unperturbed carried out by LKH is helpful in illustrating this point.)

Let us now examine the self-consistency terms in Eqs.(14a) and (14b) more carefully. We observe that in the summation the two direct terms are equal and the two exchange terms are not equal. However, in the diagrammatic representation there is only one direct term Fig. 1(h). To resolve this apparent discrepancy, let us turn to the "correlation" diagram Fig. 1(j). Now polarizability diagrams are obtained from Fig. 1 by closing the free lines with h' as indicated in Fig. 2; e.g., Fig. 1(j) becomes Fig. 2(a). Upon combining with a similar diagram Fig. 2(b), we obtain Fig. 2(c) which is identical to the self-consistency polarizability diagram obtained from Fig. 1(h).[9] Similarly Fig. 1(k) combines with its counterpart to give the first exchange term, and Fig. 1(i) accounts for the second exchange term in Eq. (14a) and (14b). Thus the polarizability diagrams obtained from Fig. 1, when summed to all orders[3,5] by the shifted-energy technique, are equivalent to the fully coupled HF method (Method a). Note that the factor of 2 coming from inverting diagrams is already accounted for in the definition of polarizability in Eq. (2). If Figs. 1(j) and 1(k) are to be interpreted as correlation, then the coupled HF method includes correlation. On the other hand, if correlation is defined as the difference between the exact and the HF approximation results, then Figs. 1(j) and 1(k) represent self-consistency and not correlation effects.

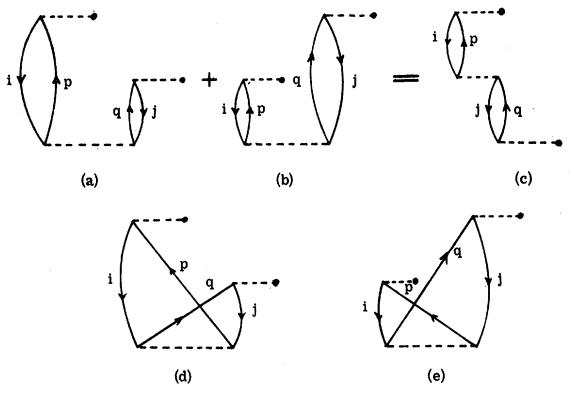

FIG. 2. Double excitation diagrams (a) and (b) and their exchange counterpart (d) and (e) that contributes to the HF perturbation theory. In particular the contribution of (a) and (b) together is equivalent to a single-excitation diagram shown in (c).

Another point of possible confusion is the treatment of doubly occupied orbitals briefly discussed by LKH. They have reformulated Method b so that the coupling terms are dropped after the doubly occupied orbitals are assumed to have the same spatial function. In other words, this formulation includes the intrashell consistency effect, and will be called Method b′. To be specific, they let

$$\varphi_i=\psi_i\alpha \quad \text{and} \quad \varphi_{i+1}=\psi_i\beta; \tag{19}$$

and Method b′ is described by

$$[f_i^{\,0}(1)-\epsilon_i]\psi_i'(1)+[h'(1)-\epsilon_i']\psi_i(1)=0, \tag{20}$$

where

$$f_i^{\,0}=T+\sum_{\substack{j=1\\ j\neq i}}^{N/2}\langle\psi_j|\frac{1}{r_{12}}(2-P_{12})|\psi_j\rangle + \langle\psi_i|\frac{1}{r_{12}}(1+2P_{12})|\psi_i\rangle\,. \tag{21}$$

In Eq. (21), the summation term on the right represents[5] the direct and exchange effects of electrons in all the doubly occupied states $j\neq i$. The last term consists of two parts, one part involving $1/r_{12}$ represents the direct interaction with the other electron in state i, while the exchange-like term arises from self-consistency effects involving the first-order perturbation of the orbital Ψ_i. In the BG approach with V^{N-1}, this intrashell consistency effect is accounted for by diagram (h) where i and j are the equivalent electrons. In this case, diagram (i) is zero because the spins are necessarily antiparallel. Since diagrams (1h) and (1j) have been found quite large in the case of beryllium by Kelly,[3] it is not clear whether the improvement of Method b′ over Method c in the polarizability results quoted by LKH is due to the inclusion of intrashell consistency or to the exclusion of the extraneous self-potential term. In the calculation of the polarizability of Li, the former is not expected to be important, and therefore V^{N-1} appears to be a more desirable choice than V^N. For this reason we have utilized the V^{N-1} potential as defined in I for the calculation of the hyperfine coupling constant and energy in lithium.

III. NUMERICAL RESULTS FOR LITHIUM

The calculation of polarizabilities and shielding factors by the Brueckner-Goldstone many-body approach has been discussed by Kelly in application to beryllium and oxygen atoms.[3,4] It is not necessary to draw both polarizability and shielding diagrams since they are identical except that one vertex H'' must be replaced by $\gamma_{\rm op}$ for the latter as is evident from the definitions Eqs. (2) and (4). To avoid double-counting, we place the restriction that $\gamma_{\rm op}$ must appear above H'', and in

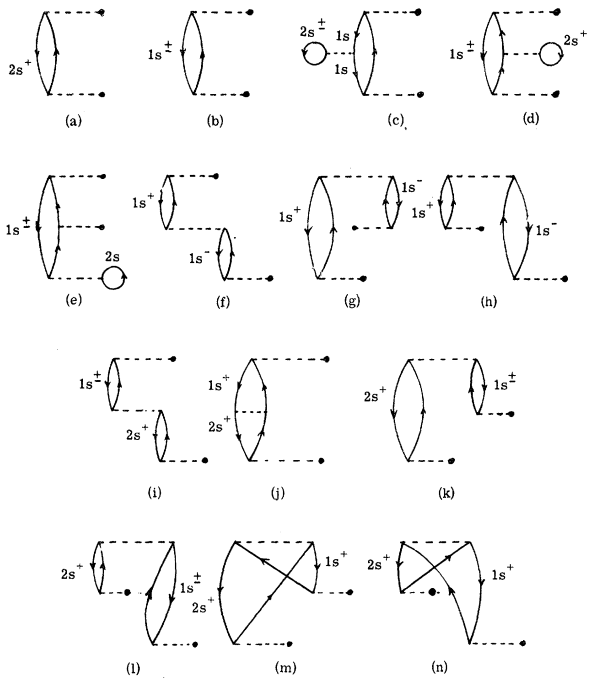

FIG. 3. Polarizability diagrams for lithium using V^{N-1} which account for intrinsic and consistency effects.

reference to a diagram the inclusion of its inverted form is implied.

As in the case of the wave-function diagrams, the polarizability diagrams given in Fig. 3 are classified according to their physical content. Thus, (a)-(e) are intrinsic diagrams, where (c), (d), and (e) arise from incomplete cancellation of the passive unexcited states with the single-particle potential V^{N-1} as defined in I. Corresponding exchange diagrams for (c), (d), and (e) are not shown, but are included in the calculation. These diagrams are to be associated with Method b. However, the Method-b results given by LKH are really Method b′ which includes just intrashell consistency effects. These are represented by diagrams (f), (g), and (h) in Fig. 3. As explained by Fig. 2. (g) and (h) add up to (f), and twice the diagram (f) is the last term in Eq. (21), representing Method b′. HF corrections similar to Fig. 3, (c) and (d) also apply to all 1s states, including diagrams (f), (g), and (h). Diagrams (i)-(n) in Fig. 3 represent intershell consistency effects which are present in Method a only. In fact, diagrams (k) and (l) add up to diagram (i), and together they account for the two direct terms in Eq. (14b). Diagram (j) represents the second exchange term which is monopole, and diagrams (m) and (n) the first exchange term which is dipole in (14b). Thus all diagrams in Fig. 3 including all HF corrections and ladders should sum up to the results of Method a.

Some higher-order diagrams[10] representing corrections to the Method a are given in Fig. 4. They are interpreted as true correlation effects, and are numerically most significant for intershell

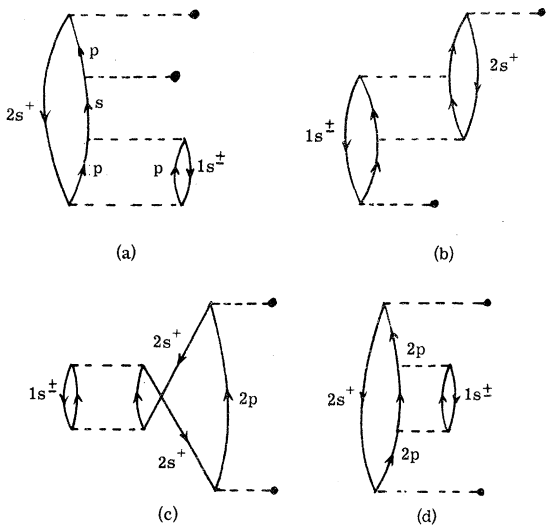

FIG. 4. Some correlation diagrams which represent improvements over Hartree-Fock perturbation methods.

correlation. If the sum of contributions from these diagrams and even higher orders is large compared with the contributions of Fig. 3, the Hartree-Fock perturbation theory is of doubtful usefulness.

In evaluating the diagrams we have used the same complete set of states as in the earlier hyperfine work. Consequently the matrix elements involving v_{ij} vertices were the same, and most of them were already available. Only matrix elements involving H'' and γ_{op} vertices need to be calculated. For example the polarizability diagrams (a) and (i) in Fig. 3 are given by (the prime indicates that summation is to be over excited states only)

$$\sum_m{}' \frac{\langle 2s|h'|m\rangle\langle m|h'|2s\rangle}{\epsilon_{2s}-\epsilon_m}$$

and

$$\sum_{n,m}{}' \frac{\langle 2s|h'|m\rangle\langle m2s|v|n1s\rangle\langle n|h'|2s\rangle}{(\epsilon_{1s}-\epsilon_m)(\epsilon_{2s}-\epsilon_n)} .$$

In Table I, we have listed the contributions to α_d and γ_d from the various diagrams discussed in the

TABLE I. Contributions to α and γ in the present calculation. Numbers in parentheses are partial results not included for the sake of consistency.

Description		α_d (Å^3)	γ_d
Intrinsic	1s	0.0321	0.845
	2s	25.031	2.752
Consistency	intrashell	−0.0042	−0.128
	intershell	−0.156	−2.508
Correlation		(0.04)	(0.015)
Total	before normalization	24.903	0.961
	after normalization	24.84 ± 0.10	0.958 ± 0.05

previous section. The effects of ladder diagrams are included by altering the energy denominators d in the second-order diagrams to $d-a$, where a is the matrix element associated with the pertinent laddering vertices.[1,3,4] Practically all of the contribution to α_d arises from the $2s$ intrinsic diagram. The result from the $1s$ orbitals is small because they are very tightly bound, or, in our perturbation language, because the excited states are well separated from the $1s$. Among the consistency diagrams, the Method b′ intershell contribution is also small for the same reason. The Method a intershell contribution from the $1s$-$2s$ interaction is relatively larger due to the stronger perturbation of the $2s$ state by the electric field. Some of the representation diagrams in fourth order are shown in Fig. 4. They represent correlation effects and are found to be unimportant. The influence of the normalization factor in Eq. (2) is small and already calculated in the hfs case. Our calculation of the polarizability gives a result of 24.84 ± 0.05 Å^3, where the uncertainty is mainly due to the approximation in calculating ladder diagrams.

For the dipole shielding factor γ_d the $2s$ intrinsic diagram makes the leading contribution although it is by no means as dominant as in the case of α. The $1s$ intrinsic contribution is now sizable because of the nature of the operator γ_{op} in (4) which emphasizes the region near the nucleus. Thus, the $2s$ diagram contributes 2.752, whereas the unmodified $1s$ diagrams contribute 0.603, and with HF corrections the latter becomes 0.845. Intrashell consistency effects in Figs. 3(f), (g), and (h) contribute −0.128, and therefore the result of our Method b′ is 3.469. Intershell consistency effects are much more important. The two direct terms represented by Fig. 3(i) and the sum of (k) and (l) each contribute −1.007, while the exchange terms (j) and the sums (m) and (n) contribute −0.097 and +0.016. In computing the effects of ladders it is easier to treat the single-particle diagrams (i) and (j) separately from the two-particle diagrams (k), (l), (m), and (n). The former change from −1.103 to −1.311 and the latter from −0.991 to −1.197.

TABLE II. Various dipole polarizability and shielding factor results for lithium.

Method	Author	α_d (Å^3)	γ_d
c	LKH[4]	7.5	1.52
d	LKH	21.0	3.61
d	S[11]	24.9	...
b′	LKH	21.0	3.62
b′	CPD	24.99	3.47
a′	LM[5]	25.2	0.988
a′	LKH	21.7	1.96
a	LKH	21.2	1.94
BG	CPD	24.84	0.958
Experimental	CZ[13]	22 ± 2	1.000
	SPB[12]	20 ± 3	1.000

Some true correlation diagrams in Fig. 4 have been examined and found to be quite small. For example Figs. 4(c) and (d) are calculated to be −0.015 and +0.015. These fourth-order diagrams are tedious to calculate and seemingly unimportant, and therefore are neglected in the present work. In the evaluation of the various diagrams, we have, of course, included the contributions from both discrete and continuum excited states. It is of some interest, however, to mention that the relative contributions to diagrams from continuum and bound excited states were different for the perturbation of $1s$ and $2s$ orbitals. For $1s$ state, over 90% of the contribution occurred from the continuum states. For $2s$ state, the presence of the adjacent $2p$ excited state made its contribution preponderant over the continuum states. In fact, for the intrinsic diagram 3(a) about 99% of the polarizability came from the $2p$ state.

IV. DISCUSSION

In Table II, we have compared our results for α_d and γ_d with the results of earlier authors and experiment. For γ_d the "experimental" value of unity is that expected from the Hellmann-Feynman theorem.[7]

Let us summarize the various methods appearing in Table II. Method a is the fully coupled Hartree-Fock perturbation method where each electron is perturbed individually. Method a′ is a slight simplification where both the $1s$ orbitals are restricted to have the same radial function. The difference is believed to be unimportant. Method b is the uncoupled approximation using V^{N-1} and retaining the intrashell consistency terms. The simplifying scheme which replaces the exchange potential in Method b by a localized potential is called Method d. Method c is a different uncoupled approximation to Method a using V^N. The BG calculation is, in principle, exact; but because the contribution of correlation diagrams in Li is smaller than the estimated accuracy, our BG results are essentially equivalent to those of Method a. From Table II we notice that identical methods by different authors may yield substantially different results. The reason is that some authors solve their equations variationally rather than numerically. Thus their results may suffer from the inflexibility of the form of their variational functions. In particular, the variational perturbed orbital used by LKH consists of the product of a polynomial and the corresponding unperturbed orbital.[5] Therefore their perturbed orbitals are constrained to have at least the same number of nodes as the unperturbed, and they are also forced to have the same exponential decaying behavior in the outer region. However, the variational perturbed orbital of Lahiri and Mukherji (LM) is more flexible in that it is a linear combination of Slater orbitals which are used to expand the corresponding unperturbed orbital.[6] The effect of using these different variational functions on the values of both α and γ_d is best illustrated by the Method a′ results. The LM value of 0.988 for γ_d as opposed to the LKH value of 1.96 speaks well for the LM variational function. Hence we might expect

that the LM value of 25.2 Å^3 for α is more reliable than the LKH value of 21.7. Support for this contention is found in the Method d results for α_d, where the LKH value of 21.0 is substantially lower than the Sternheimer (S) value of 24.9 which is obtained through solving the identical equations numerically.[11] It is therefore not surprising that the results of our Methods b′ and a are not in close agreement with the corresponding results of LKH. On the other hand, our Method a results of 24.84 for α_d and 0.958 for γ_d are in good agreement with the LM values of 25.2 and 0.988. From the Method c value for α, it is clear that our choice of V^{N-1} rather than V^N is more desirable in lithium.

Unfortunately the ranges of errors in the two recent experimental values[12,13] of (20 ± 3) and (22 ± 2) Å^3 for α are larger than both the self-consistency and correlation effects, and therefore do not permit a critical evaluation of these effects. From our results of Table I it seems unlikely that errors in the observed small self-consistency and correlation effects can remove the discrepancy between our theoretical value of 24.84 ± 0.05 Å^3 and experiment.

We also mention here three additional theoretical calculations on α_d for lithium. These have not been listed in Table II because the methods for these calculations are less amenable to direct comparison with our calculation. Dalgarno and Pengelly[14] obtained $\alpha_d = 25.6$ Å^3 using the Coulomb approximation. Stacey[15] used the Weiss 45-term configuration-interaction wave function, and thus included correlation effects. He obtained a value of 23.97 Å^3 for α_d. Using results of their calculation on the quadratic Stark effect, Murakawa and Yamamoto[16] obtained $\alpha_d = 23.9$ Å^3.

In the calculation of γ_d, the contribution of intershell consistency terms was found to be very important, while the contribution of these respective terms in α_d is relatively far less. This can be understood physically from the nature of the operator γ_{op} which emphasizes the region near the nucleus, a region where both 1s and 2s electrons contribute. Thus one expects intershell effects to be characteristically more important for γ_d as contrasted with α_d. The effect of intrashell consistency terms also contributes negligibly in the value of α_d for lithium. However, this does not necessarily mean that the intrashell consistency effect will always be small. A meaningful indication comes from the comparison in Table I of the contribution from the intrinsic 1s electrons and that from the intrashell consistency. The latter is nearly 15% of the former. Thus in atoms where there is more than one electron present in the valence band, the effect of the intrashell consistency terms could really be quite significant.

V. CONCLUDING REMARKS

We have analyzed the relation between various approximations in the Hartree-Fock perturbation method and the Brueckner-Goldstone many-body method. In particular, Method a has been found to be equivalent to the class of diagrams given in Fig. 1 (and for the case of lithium in Fig. 3). In general the polarizability is dominated by the outermost shell, so the diagrams whose contributions are comparable with Fig. 1(a) are Figs. 1(h), (i), and (j)[17] with i and j representing electrons in the outermost shell. Then Fig. 1(i) is of the same sign as Fig. 1(a) and numerically larger than Fig. 1(h) which is of opposite sign. Therefore, Method c given by Fig. 1(a) using V^N leads to an underestimation, because it neglects the dominating third-order diagram represented by Fig. 1(i) when $j=i$. On the other hand, Method b, given by Fig. 1(a) using V^{N-1} does not have Fig. 1(h) and (i) when $j=i$ and tends to overestimate, because it neglects Fig. 1(h) when electrons i and j are equivalent, which occurs for non-alkali-like atoms. This defect is removed in Method b′ which includes intraconsistency, and leads to results in close agreement with Method a. In lithium, correlation effects have been determined to be unimportant for both the dipole polarizability and shielding factor. Therefore, as expected, our results are in close agreement with the fully coupled Hartree-Fock method (LM), and also in good agreement with experiment. However, it is not clear that correlation effects are unimportant for any atom in general. It would be interesting to re-examine, from the point of view adopted in this work, the BG calculation by Kelly on beryllium,[3] where correlation and consistency effects are expected to be more important, since these effects can now occur in intrashell form between the two outer, deformable valence electrons.

In this calculation we are able to obtain good results by using only up to the second order of perturbation in the wave function. Thus, the unperturbed wave functions appear to converge quite rapidly. Indeed the calculation of the hyperfine coupling constant and the energy in I and the dipole polarizability and shielding factor here indicates that the BG wave function is good in all regions of the atom. It then appears quite feasible to calculate all atomic properties using the same set of states in the Brueckner-Goldstone approach as demonstrated for beryllium by Kelly and for lithium here.

ACKNOWLEDGMENT

One of the authors (E.S.C.) wishes to thank Professor H. P. Kelly for a very helpful discussion. We thank the Computer Center of the University of California at Riverside for the use of their facilities.

*Supported by the National Science Foundation and the National Aeronautical and Space Administration.

†National Academy of Sciences-National Research Council Resident Research Associate; present address: Laboratory for Theoretical Studies, NASA–Goddard Space Flight Center, Greenbelt, Maryland.

[1] E. S. Chang, R. T. Pu, and T. D. Das, preceeding paper [Phys. Rev. 174, 1 (1968)].

[2] J. Goldstone, Proc. Roy Soc. (London) A239, 267 (1957).

[3] H. P. Kelly, Phys. Rev. 136, B896 (1964); 131, 684 (1963).

[4]H. P. Kelly, Phys. Rev. 144, 39 (1966).
[5]P. W. Langhoff, M. Karplus, and R. P. Hurst, J. Chem. Phys. 44, 505 (1966).
[6]J. Lahiri and A. Mukherji, J. Phys. Soc. (Japan) 21, 1178 (1966).
[7]R. P. Feynman, Phys. Rev. 56, 340 (1939).
[8]E. S. Chang, Ph. D. dissertation, 1967, University of California, Riverside (unpublished).
[9]We wish to thank Professor H. P. Kelly for calling our attention to this point.
[10]A more complete list is given in Refs. 3 and 8.
[11]R. M. Sternheimer, Phys. Rev. 96, 951 (1954).
[12]A. Salop, E. Pollack, and B. Bederson, Phys. Rev. 124, 1431 (1961).
[13]G. E. Chamberlain and J. C. Zorn, Phys. Rev. 129, 677 (1963).
[14]A. Dalgarno and R. M. Pengelly, Proc. Phys. Soc. (London) 89, 503 (1966).
[15]G. M. Stacey, Proc. Phys. Soc. (London) 88, 896 (1966).
[16]K. Murakawa and M. Yamamoto, J. Phys. Soc. (Japan) 21, 821 (1966).
[17]The contribution from diagram 1(j) is comparable with that from 1(h) but does not have to be considered specifically in the subsequent discussion because it leads to diagram 2(c) which is identical with that resulting from 1(h). All remarks about the relative importance of 1(h) then apply to 1(j).

PHYSICAL REVIEW VOLUME 174, NUMBER 1 5 OCTOBER 1968

Determination of g-Factor Ratios for Free Rb^{85} and Rb^{87} Atoms*

C. W. White,† W. M. Hughes, G. S. Hayne, and H. G. Robinson
Duke University, Durham, North Carolina
(Received 6 May 1968)

The ratio of the nuclear g factor to the electronic g factor in the ground electronic state of free $Rb^{85,87}$ atoms has been determined using optical pumping techniques in a magnetic field of ≤ 50 G. Typical linewidths were ≤ 15 cps. The linewidth contribution due to magnetic field effects was less than 1 cps. The ratio of electronic g factors for the Rb isotopes was also measured. The results are $-g_I/g_J(Rb^{87}) = 4.969\,914\,7 \times (1 \pm 0.9 \times 10^{-6}) \times 10^{-4}$, $-g_I/g_J(Rb^{85}) = 1.466\,490\,8 \times (1 \pm 2.1 \times 10^{-6}) \times 10^{-4}$, and $g_J(Rb^{87})/g_J(Rb^{85}) = 1.000\,000\,004\,1 \times (1 \pm 6.0 \times 10^{-9})$. These results were obtained from evacuated wall-coated cells having the Lorentzian line shape. Cells filled with inert buffer gases exhibited small, uncontrollable, systematic error due to non-Lorentzian line shape. In both types of cells, the Zeeman resonances exhibited frequency shifts proportional to the pumping-light intensity. The ratio $g_I(Rb^{85})/g_I(Rb^{87}) = 0.295\,073\,6 \times (1 \pm 2.3 \times 10^{-6})$ was obtained by combining the results above. The combination with results of other researchers yields the chemical shift of Rb^+ in aqueous solution relative to the free atom as $\Delta\sigma(Rb^+_{aq}/Rb) = -(211.6 \pm 1.2) \times 10^{-6}$. Absolute values in units of the Bohr magneton for the shielded nuclear moments are derived using only g-factor ratios for free atoms: $g_I(Rb^{87}) = -0.995\,141\,4 \times 10^{-3} \times (1 \pm 1.0 \times 10^{-6})$ and $g_I(Rb^{85}) = -0.293\,6400 \times 10^{-3} \times (1 \pm 2.2 \times 10^{-6})$.

I. INTRODUCTION

The basic motivation for this work followed from the desire to measure ground-electronic-state alkali g_J ratios to high precision using optical-pumping techniques incorporating the advantages of wall-coated evacuated cells. Earlier efforts[1] using the Rb isotopes were limited in resolution primarily by the applied magnetic field. The work to be reported in this paper is unique in enjoying a field improved beyond the point where it contributed significantly to the system resolution. In experiments using this improved apparatus, when the then-latest atomic-beam[2] determination for $g_I/g_J(Rb^{85})$ was used in the Breit-Rabi equation to fit experimental data, the g_J value derived from $\Delta F = 0$ Zeeman transitions in the $F = 3$ level complex differed significantly from the value for the $F = 2$ level complex. Accordingly, our experiment was inverted to determine the g_I/g_J ratios for the Rb isotopes. Following publication of preliminary results,[3] two other experiments[4,5] were initiated whose results confirmed our conclusion that the earlier $g_I/g_J(Rb^{85})$ value was in error. This paper reports the final results for our measurement of g_I/g_J in $Rb^{85,87}$ and of $g_J(Rb^{85})/g_J(Rb^{87})$. The high resolution of the experiment permitted the first observation of shifts in the $\Delta F = 0$ Zeeman transitions of Rb induced by the pumping light.

II. THEORY

The energy levels of the $^2S_{1/2}$ electronic state of an alkali atom in an applied magnetic field, $\vec{H}$, are assumed to be represented by the effective Hamiltonian

$$\mathcal{H} = ha\vec{I}\cdot\vec{J} + g_J\mu_0\vec{J}\cdot\vec{H} + g_I\mu_0\vec{I}\cdot\vec{H} \qquad (1)$$